

Quantitative structure–selectivity relationship for M2 selectivity between M1 and M2 of piperidinyl piperidine derivatives as muscarinic antagonists

Yin-Yao Niu,^a Li-Min Yang,^a Ke-Min Deng,^a Jian-Hua Yao,^{b,*} Liang Zhu,^a
Cong-Ying Chen,^a Min Zhang,^a Jin-E Zhou,^a Tian-Xiang Shen,^b
Hong-Zhuan Chen^a and Yang Lu^{a,*}

^aDepartment of Pharmacy, Shanghai Jiao Tong University School of Medicine, Shanghai 200025, China

^bShanghai Institute of Organic Chemistry, Chinese Academy of Sciences, Shanghai 200032, China

Received 29 October 2006; revised 14 January 2007; accepted 19 January 2007

Available online 25 January 2007

Abstract—Muscarinic M2 receptor antagonists with high subtype selectivity (M2/M1) will decrease the toxicity in central nervous system in treatment of AD. The exploration of quantitative structure–selectivity relationship (QSSR) to muscarinic M2 receptor antagonists will provide design information for drug with fewer side effects. In this paper, CoMFA models of $pK_i(M1)$, $pK_i(M2)$ and $p[K_i(M2)/K_i(M1)]$ ($pK_i(M2) - pK_i(M1)$) were used to study the subtype selectivity (M2/M1) of piperidinyl piperidine derivatives as muscarinic M2 subtype receptor antagonists. The parameters of the three models are: 0.633, 0.636 and 0.726 for cross-validated r^2 (r_{cv}^2), 0.109, 0.204 and 0.09 for the Standard error of estimate (SD), respectively. The results show the model of $p[K_i(M2)/K_i(M1)]$ is the best one for design of piperidinyl piperidine derivatives as muscarinic antagonists with high subtype selectivity (M2/M1).

© 2007 Elsevier Ltd. All rights reserved.

Alzheimer's disease (AD), clinically characterized by a noticeable cognitive decline defined by a loss of memory and learning ability, is due in part to the impairment of the cholinergic function. One of the consistent findings in brains of AD patients is the declining level of acetylcholine (ACh), the muscarinic endonative agonist mediated cognitive effects by stimulating the postsynaptic muscarinic M1 receptors in central nervous system. Since muscarinic M2 subtype receptor antagonists could increase ACh release and improve learning ability through its blockade of the presynaptic M2 autoreceptors in the brain, the development of muscarinic M2 subtype receptor antagonists becomes one of the cholinergic approaches to AD by improving ACh level.^{1,2} As muscarinic M1 receptors mediate the ACh effect, the muscarinic antagonists with high subtype selectivity to M2 receptor versus M1 one would increase the cholinergic

transmission with fewer side effects in the therapeutic use. However, the muscarinic M2 subtype receptor antagonists of practical interest have not been produced partially because of their insufficient subtype selectivity (M2/M1).

Some of 3D mathematic analytical methods, such as comparative molecular field analysis (CoMFA),³ have been widely applied in studying the quantitative structure–activity relationship (QSAR) and provided the useful information to understand the relationship between structure and activity.^{4,5} Lots of successful examples in QSAR prompted us to consider whether the quantitative mathematic protocols also could be effective in the study of muscarinic subtype selectivity (M2/M1) to aid the design of muscarinic M2 subtype receptor antagonists for clinical purpose. In fact, various quantitative analytical methods have been applied in the selectivity of ligand to receptors or subtypes of the receptors,^{6,7} and understanding the quantitative structure–selectivity relationship (QSSR) is crucial for improving the subtype selectivity. However, muscarinic subtype M2 antagonists have been rarely investigated with QSSR. This paper will present the work about this by applying a

Keywords: QSSR; CoMFA; Muscarinic antagonists; Subtype selectivity.

* Corresponding authors. Tel.: +86 21 63846590 776464; fax: +86 21 53065329 (Y.L.); tel.: +86 21 54925264; fax: +86 21 64166128 (J.-H.Y.); e-mail addresses: yaojh@mail.sioc.ac.cn; huaxue@shsmu.edu.cn

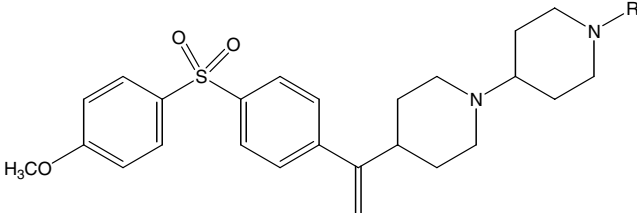
series of piperidinyl piperidine derivatives as muscarinic M2 subtype receptor antagonists which were synthesized and studied pharmacologically by Wang YG group.⁸ As the difference among the subtype selectivity (M2/M1) values of these compounds is obvious and some compounds show satisfactory subtype selectivity (M2/M1), we thought these compounds were quite worth discussed by QSSR. The ratio of $K_i(\text{M2})$ to $K_i(\text{M1})$ for muscarinic antagonist, defined usually as the subtype selectivity (M2/M1) and in fact, is largely dependent upon its structure. According to the principle of CoMFA, QSSR study for selectivity of muscarinic subtype M2 antagonists could be carried out following two approaches respectively.

Comparison of CoMFA model of $pK_i(\text{M1})$ with that of $pK_i(\text{M2})$. In the process of QSAR study with CoMFA to a series of muscarinic M1 or M2 receptor antagonists, which usually possess identical molecule-skeleton and relative geometry and interact with the same target (receptor, enzyme, ion channel or transporter) in the same manner, a set of suitable conformations of these molecules with identical orientations in space are superimposed based on a rational alignment rule (such as a pharmacophore hypothesis). Then, different atomic probes are used to calculate the steric and electrostatic fields of these molecules. These fields corresponding to tables are correlated with negative logarithm of the binding affinities ($pK_i(\text{M1})$ ($-\log(K_i(\text{M1}))$) or $pK_i(\text{M2})$ ($-\log(K_i(\text{M2}))$) for muscarinic antagonists against M1 or M2 receptor) which are applied as the dependent variable in the partial least squares (PLS) analysis of CoMFA. The steric and electrostatic contour plots presented by the validated analytical result will show favourable and unfavourable regions around the molecules in steric as well as in electrostatic. If the steric or electrostatic polyhedrons of the validated CoMFA models of $pK_i(\text{M1})$ and $pK_i(\text{M2})$ (the models were named after the dependent variable for convenience) appear in the same regions of the molecules and display contrary steric and electrostatic features (for example, the red polyhedron in the electrostatic and green one in the steric contours of CoMFA model of $pK_i(\text{M2})$, while the blue and yellow ones for of $pK_i(\text{M1})$ appear in the same region of the molecule), we could deduce that an increase of electron density or steric bulk in this region will improve the $pK_i(\text{M2})$ values and reduce the $pK_i(\text{M1})$ values by comparing the two contours. Then, the structural information of improving the muscarinic subtype selectivity (M2/M1) ($p[K_i(\text{M2})] - p[K_i(\text{M1})]$) could be acquired explicitly. In fact, the selected molecular conformation for alignment in building CoMFA model plays an important role in determining the position of the contours and the validation of the CoMFA model. In general, applying one set of conformation for the CoMFA studies would be beneficial to satisfy the requirement for the polyhedrons of CoMFA models of $pK_i(\text{M1})$ and $pK_i(\text{M2})$ appearing in the same regions and being compared effectively. However, whether CoMFA models of $pK_i(\text{M1})$ and $pK_i(\text{M2})$ constructed in one set of conformation are both validated remains unclear. In constructing CoMFA models of $pK_i(\text{M1})$ and $pK_i(\text{M2})$ as two separate dependent variables, we

found it difficult that the r_{cv}^2 values of the two quantitative equations constructed in one set of conformation could both be greater than 0.5 (generally, the r_{cv}^2 value for a validated model is greater than 0.5). Thus, we employed two sets of conformations in practically building validated CoMFA models of $pK_i(\text{M1})$ and $pK_i(\text{M2})$, and expected to get some useful structural information for increasing the muscarinic subtype selectivity (M2/M1) by comparing their steric and electrostatic contour maps.

Nineteen piperidinyl piperidine derivatives are divided into a training set (compounds marked with ‘†’) and a test set, their binding affinities ($K_i(\text{M1})$, $K_i(\text{M2})$) against muscarinic M1, M2 subtype receptors, and the ratios of $K_i(\text{M2})$ to $K_i(\text{M1})$ are listed in Table 1. The CoMFA models of $pK_i(\text{M1})$ and $pK_i(\text{M2})$ were performed on a Silicon Graphics workstation using Sybyl (version 6.9).⁹ The structures of all compounds in Table 1 were input by SYBYL/SKETCH procedure. Structural energy minimization of each compound was treated by the standard Tripos molecular mechanics force field with a 0.05 kcal/mol energy gradient convergence criterion and a distance-dependent dielectric constant (max iteration = 3000). Charges were calculated by the Gasteiger–Hückel method, the conformation search was finished by multiple conformational searches. Two sets of conformations of targeted compounds were employed in the two CoMFA models, respectively. The alignment rule selected in CoMFA is often critical to the analytical result. In our case, two phenyl groups and two N atoms in the compounds were selected as the fitting centres marked with asterisk (*) in alignment (Fig. 1), because they were very critical to the binding affinity against muscarinic M1 or M2 subtype receptor.^{8,10–13} For the alignment, all aligned compounds were superimposed using an atom-by-atom least square. Compound 4 was selected as template in the SYBYL Fit option due to its highest subtype selectivity (M2/M1) and higher binding affinities against muscarinic M1 and M2 subtype receptors. The aligned molecules were put into a 3D grid with a distance-dependent constant spacing of 2 Å, and sp^3 carbon probe atom with +1 charge was used to estimate the steric and electrostatic fields. Values of the steric and electrostatic energies were truncated at 30 kcal/mol. The $pK_i(\text{M1})$ or $pK_i(\text{M2})$ was, respectively, employed as the dependent variable and regression analysis of the resulting matrix was performed by PLS linear regression for the training set. To speed up the PLS analysis and reduce noise, column filtering was set at 2.0 kcal/mol. The optimal number of components (N) was employed to do no validated PLS analysis to get the conventional correlation coefficient (r^2) and the cross-validated r^2 (r_{cv}^2) of the training set determined by a leave-one-out (LOO) was applied for the validation of the two CoMFA models following the general understanding of this method. The compounds of test set were utilized for external model validation.

Analysis of steric and electrostatic contours of validated CoMFA model of $p[K_i(\text{M2})/K_i(\text{M1})]$ ($-\log(K_i(\text{M2}))$) ($-\log(K_i(\text{M1}))$). Lots of studies about the binding sites of diverse muscarinic subtype receptors by simulating the

Table 1. Structures of piperidinyl piperidine derivatives, associated binding affinities ($K_i(M1)$, $K_i(M2)$) and subtype selectivity (M2/M1) ($K_i(M2)/K_i(M1)$)


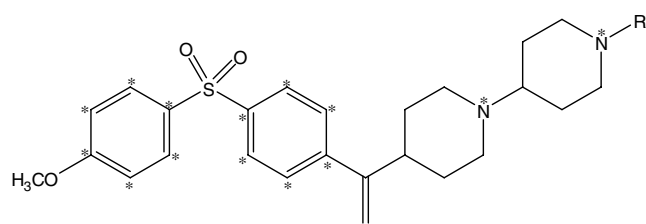
Compound	R	Binding affinity (K_i , nM)		Subtype selectivity (M2/M1)	
		$K_i(M1)^b$	$K_i(M2)^a$	$K_i(M1)/K_i(M2)^a$	$K_i(M2)/K_i(M1)^c$
1 [†]	H	9.1	1.14	8	0.125
2 [†]	CO–Et	60.8	3.8	16	0.063
3	CO– <i>n</i> -C ₃ H ₇	42.18	0.38	111	0.009
4 [†]	CO–cyclopropyl	68.12	0.26	262	0.004
5 [†]	CO– <i>i</i> -C ₃ H ₇	116.6	2.2	53	0.019
6 [†]	CO–CH ₂ Ph	95.68	2.99	32	0.031
7	SO ₂ –Et	74.52	0.46	162	0.006
8 [†]	SO ₂ – <i>n</i> -C ₃ H ₇	25.81	0.29	89	0.011
9 [†]	SO ₂ – <i>i</i> -C ₃ H ₇	31.68	0.16	198	0.005
10 [†]	SO ₂ – <i>n</i> -C ₄ H ₉	57	0.38	150	0.007
11	SO ₂ –Ph	37.44	0.36	104	0.010
12 [†]	SO ₂ –CH ₂ Ph	33.35	1.45	23	0.044
13 [†]	COO–Me	60.39	0.99	61	0.016
14 [†]	COO–Et	6.49	0.11	59	0.017
15 [†]	COO– <i>n</i> -C ₃ H ₇	40.71	0.59	69	0.015
16	COO– <i>i</i> -C ₃ H ₇	14.76	0.41	36	0.028
17 [†]	COO– <i>n</i> -C ₄ H ₉	9.8	0.35	28	0.036
18 [†]	COO– <i>i</i> -C ₄ H ₉	10.5	0.30	35	0.029
19 [†]	COO–CH ₂ Ph	10.8	0.45	24	0.042

^a From Ref. 8.

^b $K_i(M1)$ values were calculated from data $K_i(M2)$ and $K_i(M1)/K_i(M2)^a$.

^c $K_i(M2)/K_i(M1)$ values were calculated from data $K_i(M1)/K_i(M2)^a$.

[†] In training set.

**Figure 1.** Structure of piperidinyl piperidine derivatives.

interaction between ligand and receptor, applying site-directed mutagenesis skills,^{14,15} have indicated that these subtypes of muscarinic receptor share a common binding pocket^{16,17} which was mainly composed of the conserved residues in transmembranes (TMs) 3, 4, 5, 6 and 7.^{18,19} Some muscarinic antagonists with intermediate dimension could partially get into this binding pocket. The inner part (within the pocket) of the molecule could bind with the conserved residues in TM regions, while the outer part (outside the pocket) with the non-conserved in some intracellular loops (such as e2 loops), by steric and electrostatic interactions.¹⁶ The common features of interactions between the inner part of the muscarinic antagonist and the conserved residues in TM regions of muscarinic M1 or M2 receptors resulted in less subtype selectivity (M2/M1) of muscarinic antagonists. Whereas, the various fea-

tures of the interactions between the outer part of the muscarinic antagonist and the non-conserved residues in the loop regions of muscarinic M1 or M2 subtype receptors might contribute to the subtype selectivity (M2/M1) and display the difference between the binding affinity ($K_i(M1)$) and that ($K_i(M2)$). The regularity and half-rigidity of the α -helix structure in the TM regions prompt the 3D-structures of the binding pockets being highly conserved. The conserved pocket regulates the same binding conformation and its orientation for the muscarinic antagonist in its binding with muscarinic M1, M2 subtype receptors. The agreement of conformation and orientation selected for the muscarinic antagonist in binding with the two muscarinic subtype receptors, along with the identical orientation in space for the series of muscarinic antagonists with common molecular skeleton, provides rational structural basis for directly studying the quantitative relationship between the subtype selectivity (M2/M1) of muscarinic antagonists and their structures with CoMFA. Following this expectation, the negative logarithm of the ratio of $K_i(M2)$ to $K_i(M1)$ ($p[K_i(M2)/K_i(M1)]$) was used as the dependent variable in building the CoMFA model of $p[K_i(M2)/K_i(M1)]$. The CoMFA manipulate followed the above studies to the CoMFA models of $pK_i(M1)$ and $pK_i(M2)$. The M2/M1 subtype selectivity was observed by the CoMFA model of $p[K_i(M2)/K_i(M1)]$ based on an interesting QSSR study.

Table 2. CoMFA analytical results about binding affinities ($K_i(M1)$, $K_i(M2)$) and subtype selectivity (M2/M1) ($K_i(M2)/K_i(M1)$) of piperidinyll piperidine derivatives

Dependent variable	$pK_i(M1)^a$	$pK_i(M2)^b$	$p[K_i(M2)/K_i(M1)]^c$
Cross-validated r^2 (r_{cv}^2)	0.633	0.636	0.726
Standard error of estimate (SD)	0.109	0.204	0.09
Conventional r^2	0.944	0.835	0.967
Optimal component (N)	3	2	4
F value	62.38	30.34	72.14
Relative steric contribution	0.451	0.498	0.358
Relative electrostatic contribution	0.549	0.502	0.642

^a $pK_i(M1) = -\log K_i(M1)$.^b $pK_i(M2) = -\log K_i(M2)$.^c $p[K_i(M2)/K_i(M1)] = pK_i(M2) - pK_i(M1)$.

All parameters of the three CoMFA models of $pK_i(M1)$, $pK_i(M2)$ and $p[K_i(M2)/K_i(M1)]$ are listed in Table 2. The optimum values of cross-validated r^2 (r_{cv}^2) are 0.633 ($N = 3$), 0.636 ($N = 2$) and 0.726 ($N = 4$), respectively. The values of conventional r^2 are 0.944, 0.835 and 0.967. In the analyses of CoMFA models of $pK_i(M1)$ and $pK_i(M2)$, the standard errors and F values are 0.109, 0.204 and 62.38, 30.34, while in that of CoMFA model of $p[K_i(M2)/K_i(M1)]$, 0.09 and 72.14. The relative contributions of steric and electrostatic fields are almost identical in the CoMFA models of $pK_i(M1)$ and $pK_i(M2)$, while the relative contributions of steric and electrostatic fields are 64.2% and 35.8%, respectively, in the CoMFA model of $p[K_i(M2)/K_i(M1)]$, indicating that the $p[K_i(M2)/K_i(M1)]$ value largely depends on the electrostatic field. The predicted values of $pK_i(M1)$, $pK_i(M2)$ and $p[K_i(M2)/K_i(M1)]$ and their residuals of the analyzed compounds by the three CoMFA models are listed in Table 3. Figures 2a–c show three effective plots of predicted $pK_i(M1)$, $pK_i(M2)$ and $p[K_i(M2)/K_i(M1)]$ versus observed ones for the training set. All

the three resultant CoMFA models had fair predictive abilities.

The steric and electrostatic fields based on PLS analysis are represented as 3D contour maps in Figures 3–6. In Figures 3a, b and 5, the green regions indicate areas where steric bulk enhances the binding affinities of targeted compounds against the muscarinic M1 and M2 receptors and subtype selectivity (M2/M1), while the yellow regions the less steric bulk is favoured to the binding affinities and subtype selectivity (M2/M1). In Figures 4a, b and 6, the blue regions indicate areas where electro-positive groups enhance binding affinities and subtype selectivity (M2/M1), while the red regions electronegative groups enhance binding affinities and subtype selectivity (M2/M1).

In Figures 3a and b, a large green polyhedron appears in the same lower regions of the substituted R group which is in the right part of the molecules, and the polyhedrons in the upper regions are all yellow. The agreement of the

Table 3. Observed and predicted negative logarithm of the binding affinities ($K_i(M1)$, $K_i(M2)$) and subtype selectivity (M2/M1) [$K_i(M2)/K_i(M1)$] of piperidinyll piperidine derivatives by the three CoMFA models

Compound	$pK_i(M1)$			$pK_i(M2)$			$p[K_i(M2)/K_i(M1)]$		
	(Obs.)	(Pred.)	Res.	(Obs.)	(Pred.)	Res.	(Obs.)	(Pred.)	Res.
<i>Training set</i>									
1	8.041	7.969	0.072	8.943	8.877	0.066	0.903	0.894	0.009
2	7.216	7.220	-0.004	8.420	8.378	0.042	1.204	1.205	-0.001
4	7.167	7.059	0.108	9.585	9.544	0.041	2.418	2.416	0.002
5	6.933	7.051	-0.118	8.658	8.731	-0.073	1.724	1.719	0.005
6	7.019	7.040	-0.021	8.524	8.463	0.061	1.505	1.522	-0.017
8	7.588	7.475	0.113	9.538	9.516	0.022	1.949	2.077	-0.128
9	7.499	7.373	0.126	9.796	9.636	0.16	2.297	2.347	-0.050
10	7.244	7.403	-0.159	9.420	9.515	-0.095	2.176	2.083	0.093
12	7.477	7.466	0.011	8.839	8.885	-0.046	1.362	1.400	-0.038
13	7.219	7.241	-0.022	9.004	9.396	-0.392	1.785	1.723	0.062
14	8.188	8.039	0.149	9.959	9.479	0.48	1.771	1.727	0.044
15	7.390	7.422	-0.032	9.229	9.452	-0.223	1.839	1.661	0.178
17	8.009	8.137	-0.128	9.456	9.447	0.009	1.447	1.533	-0.086
18	7.979	8.059	-0.08	9.523	9.471	0.052	1.544	1.549	-0.005
19	7.967	7.981	-0.014	9.347	9.446	-0.099	1.380	1.461	-0.081
<i>Test set</i>									
3	7.375	7.161	0.214	9.420	9.507	-0.087	2.045	2.216	-0.171
7	7.128	7.365	-0.237	9.337	9.494	-0.157	2.210	2.176	0.034
11	7.427	7.344	0.083	9.444	9.302	0.142	2.017	2.022	-0.005
16	7.831	7.894	0.072	9.387	9.475	0.066	1.556	1.765	-0.209

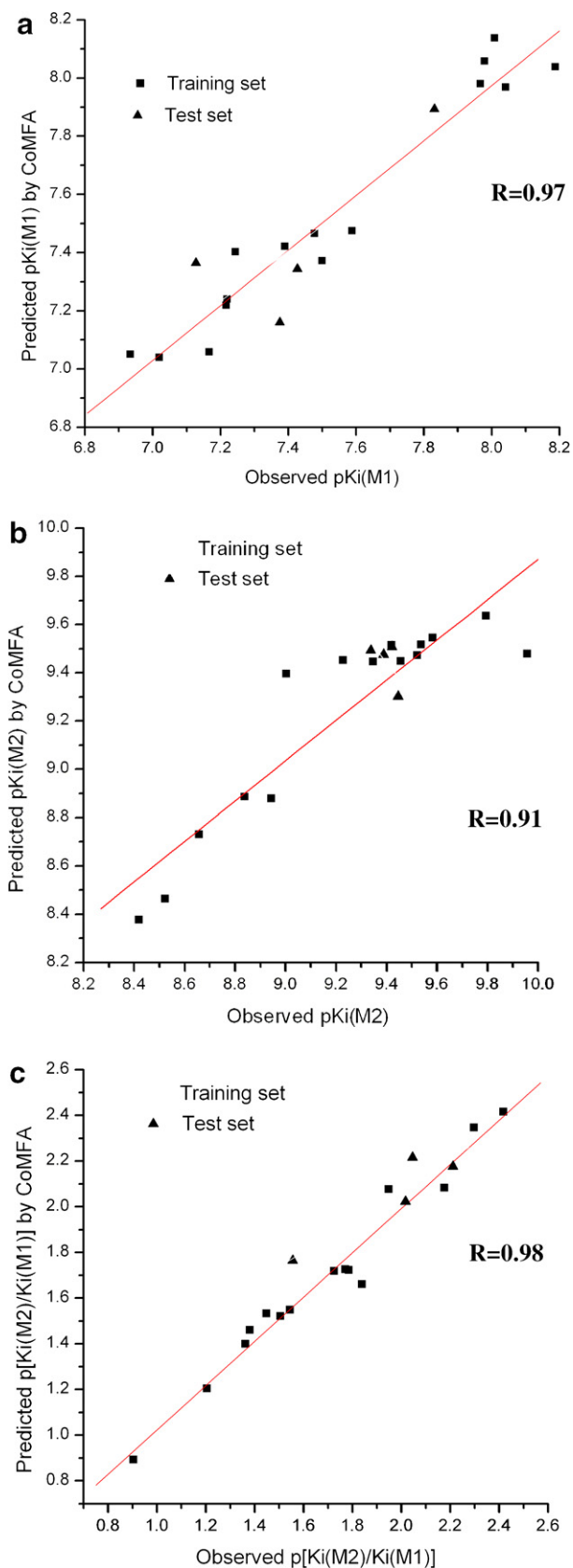


Figure 2. Predicted versus observed negative logarithm of (a) binding affinity ($K_i(M1)$) (b) binding affinity ($K_i(M2)$) (c) subtype selectivity ($K_i(M2)/K_i(M1)$) for the training set derived from the three CoMFA models, respectively.

feature of steric contour polyhedrons in the same regions surrounding the substituted R group could not provide us the effective steric information of the structure for increasing the subtype selectivity (M2/M1). But, the largest green polyhedron in the regions of the substituted R group in Figure 5 directly indicates steric bulk of the R group enhances subtype selectivity (M2/M1) as a whole. The compound **1** with the least steric bulky substituted H atom, in the training set obviously has the lowest subtype selectivity (M2/M1) ($p[K_i(M2)/K_i(M1)] = 0.903$).

The upper regions of the substituted R group regions display red polyhedron in Figure 4a and blue one in Figure 4b, indicating that the positive charge in the regions will increase $pK_i(M2)$ values, meanwhile decreasing the $pK_i(M1)$ values. It could be deduced that the positive charge in this region will increase the subtype selectivity (M2/M1). The result is in good agreement with that acquired directly from Figure 6 in which the large blue electrostatic polyhedron in the upper regions of the R group provides identical structural clues for increasing the subtype selectivity (M2/M1). It is elucidated by the observed $p[K_i(M2)/K_i(M1)]$ values that **10** ($p[K_i(M2)/K_i(M1)] = 2.176$) with sulfonyl in R group, which strongly withdraws electron, has higher value of $p[K_i(M2)/K_i(M1)]$ than that of its carbonate derivative **17** ($p[K_i(M2)/K_i(M1)] = 1.447$). Identically, by comparing the polyhedrons in the same lower regions of the substituted R group in Figures 4a and b, we could conclude that negative charge in the regions would be beneficial to the subtype selectivity (M2/M1) in the light of above analytical protocol. This result could also be suggested by the red polyhedron appearing in the same regions of substituted R group in Figure 6.

In Figures 5 and 6, one small yellow polyhedron near the position of carbonyl or sulfonyl in substituted R group indicates areas where steric bulk would modestly lower the muscarinic subtype selectivity (M2/M1). According to this suggestion, the compound with sulfonyl in the R group should have less subtype selectivity (M2/M1) than that of its carbonyl derivative. Whereas the sulfonyl group has higher ability of withdrawing electron than the carbonyl group theoretically and is beneficial to the subtype selectivity (M2/M1) of the compound referred to in the electrostatic field discussion above. These contradictory suggestions indicate that the substitution effect should be a little complicated. Considering the electrostatic contribution to the subtype selectivity is 64.2%, we speculate that the electrostatic factor should control the subtype selectivity (M2/M1). It is well elucidated by the fact that **9** ($p[K_i(M2)/K_i(M1)] = 2.297$) with sulfonyl group has higher selectivity than that of **5** ($p[K_i(M2)/K_i(M1)] = 1.724$) with carbonyl group. Nevertheless, that the selectivity of sulfonyl **8** ($p[K_i(M2)/K_i(M1)] = 1.949$) with sulfonyl group is weaker than that of its carbonyl derivative **3** ($p[K_i(M2)/K_i(M1)] = 2.045$) indicates that the steric factor should not be underestimated to some extent. Furthermore, *i*-C₃H₇, in the R group of **5**, **9**, **16**, was more bulky and electron-donating than *n*-C₃H₇, in the R group of **3**, **8**, **15**. The bulky effect would be beneficial

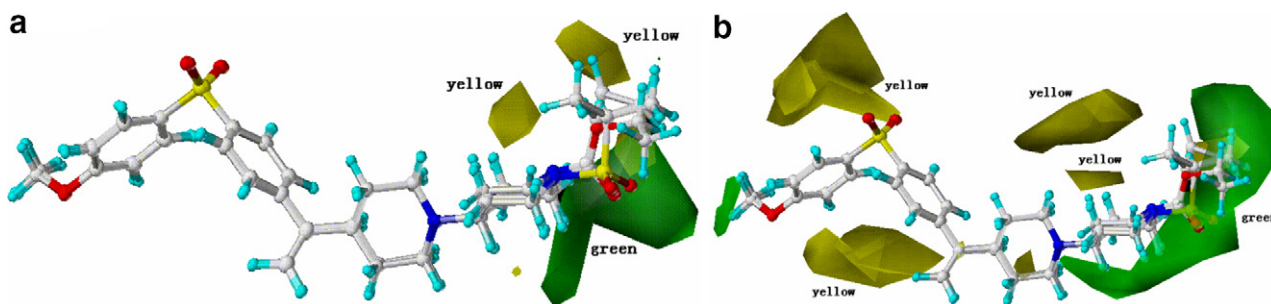


Figure 3. CoMFA SD * coeff. steric contour plots; green represents regions where steric bulk is predicted to increase binding affinity, and yellow represents regions where an increase of steric bulk is predicted to decrease binding affinity. The template **4**, compounds **9** and **17** are displayed to aid interpretation. (a) for $pK_i(M1)$ values (b) for $pK_i(M2)$ values.

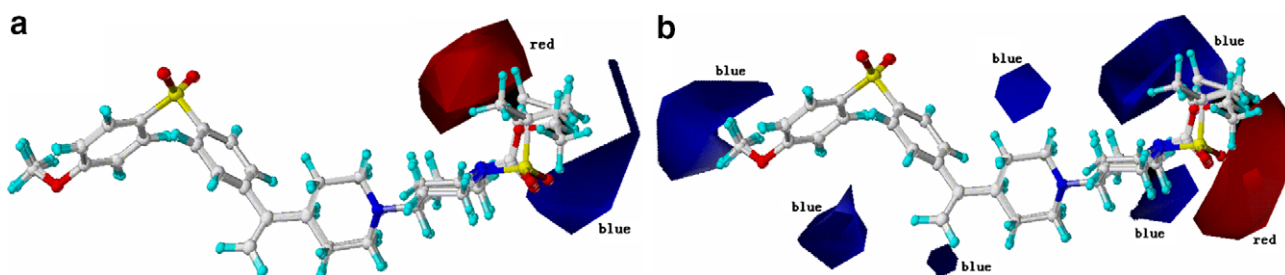


Figure 4. CoMFA SD * coeff. electrostatic contour plots; red contours represent regions where high electron density (negative charge) is expected to increase binding affinity, and blue contours represent regions where low electron density (partial positive charge) is predicted to increase binding affinity. The template **4**, compounds **9** and **17** are displayed to aid interpretation. (a) For $pK_i(M1)$ values (b) for $pK_i(M2)$ values.

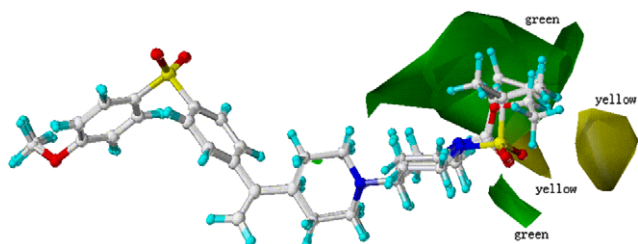


Figure 5. CoMFA SD * coeff. steric contour plots; green represents regions where steric bulk is predicted to increase muscarinic subtype selectivity (M2/M1), and yellow represents regions where an increase of steric bulk is predicted to decrease muscarinic subtype selectivity (M2/M1). The template **4**, compounds **9** and **17** are displayed to aid interpretation.

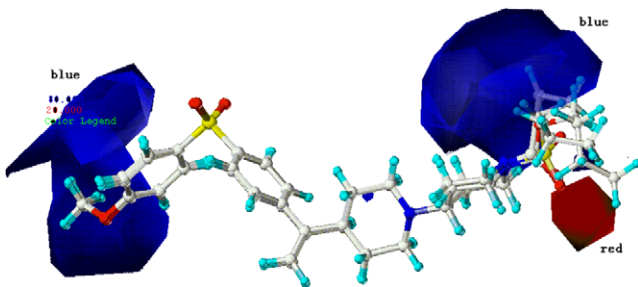


Figure 6. CoMFA SD * coeff. electrostatic contour plots; red contours represent regions where high electron density (negative charge) is expected to increase muscarinic subtype selectivity (M2/M1), and blue contours represent regions where low electron density (partial positive charge) is predicted to increase muscarinic subtype selectivity (M2/M1). The template **4**, compounds **9** and **17** are displayed to aid interpretation.

to the subtype selectivity (M2/M1) of **5**, **9**, **16**, whereas the electron-donating effect by influencing sulfonyl ($-\text{SO}_2$), carbonyl ($-\text{CO}$) and esteryl ($-\text{COO}$) groups would decrease that of **5**, **9**, **16** according to above discussions. However, the influence of $i\text{-C}_3\text{H}_7$ and $n\text{-C}_3\text{H}_7$ groups to the electrostatic effects of $-\text{SO}_2$, $-\text{CO}$ and $-\text{COO}$ groups may be different. The subtype selectivity (M2/M1) of compound **9** ($\text{SO}_2\text{-}i\text{-C}_3\text{H}_7$, $p[K_i(M2)/K_i(M1)] = 2.297$) was higher than that of **8** ($\text{SO}_2\text{-}n\text{-C}_3\text{H}_7$, $p[K_i(M2)/K_i(M1)] = 1.949$), whereas the selectivity of compounds **5** ($\text{CO-}i\text{-C}_3\text{H}_7$, $p[K_i(M2)/K_i(M1)] = 1.724$) and **16** ($\text{COO-}i\text{-C}_3\text{H}_7$, $p[K_i(M2)/K_i(M1)] = 1.556$) was lower than that of **3** ($\text{CO-}n\text{-C}_3\text{H}_7$, $p[K_i(M2)/K_i(M1)] = 2.045$) and **15** ($\text{COO-}n\text{-C}_3\text{H}_7$, $p[K_i(M2)/K_i(M1)] = 1.839$). This means that the influence of electron-donating effect of $i\text{-C}_3\text{H}_7$ and $n\text{-C}_3\text{H}_7$ groups to the electrostatic effect of $-\text{SO}_2$ groups is weak, but to $-\text{CO}$ and $-\text{COO}$ groups crucial.

According to the above discussions on Figures 3 and 4, the steric information for improving the subtype selectivity (M2/M1) by comparing the two steric contour maps of CoMFA models of $pK_i(M1)$ and $pK_i(M2)$ could not be derived. Whereas, the electrostatic features of increasing the subtype selectivity by comparing their electrostatic contour maps are acquired and the analytical result is in good agreement with that directly concluded from the electrostatic contour map of CoMFA model of $p[K_i(M2)/K_i(M1)]$ (Fig. 6). This indicates that the protocol of acquiring the structural clues for improving the selectivity by comparing the two 3D contour plots is a little complicated and could not be completely excluded in practical QSSR studies.

We have successfully constructed three validated CoMFA models of $pK_i(M1)$, $pK_i(M2)$ and $p[K_i(M2)/K_i(M1)]$ in the case of employing three diverse sets of conformation of piperidinyl piperidine derivatives as muscarinic receptor antagonists. All of the three models had good statistical results in terms of r_{cv}^2 values and proved good predictive abilities. The contour diagrams of CoMFA model of $p[K_i(M2)/K_i(M1)]$ obtained for the field contribution could gain insight into the influence of their steric and electrostatic properties on the subtype selectivity (M2/M1) and account for the muscarinic subtype selectivity (M2/M1) trend among the analyzed molecules. The analytical result provided the basis for the screening of muscarinic M2 subtype receptor selective antagonists. The quantitative analytical methodology described herein for QSSR study by CoMFA may be applied in many other medicinal studies.

Acknowledgments

We present our grateful thanks to Municipal Science Emphasis Item (No. 34319230), Ministry of Science and Technology of China (MOST) Item (No. 2002AA231011), National Natural Science Foundation of China (NSFC) Item (Nos. 20473112 and 30672441) and Shanghai Municipal Science Item (Nos. 05ZR14054 and 044307036) for financial support.

References and notes

- Greenlee, W.; Clader, T.; Asberom, T.; McCombie, S.; Ford, J.; Guzik, H.; Kozlowski, J.; Li, S.; Liu, C.; Lowe, D.; Vice, S.; Zhao, H.; Zhou, G.; Billard, W.; Binch, H.; Crosby, R.; Duffy, R.; Lachowicz, J.; Coffin, V.; Watkins, R.; Ruperto, V.; Strader, C.; Taylor, L.; Cox, K. *II Farmaco* **2001**, *56*, 247.
- Camps, P.; Torrero, D. M. *Mini-Rev. Med. Chem.* **2002**, *2*, 11.
- Cramer, R. D., III; Patterson, D. E.; Bunce, J. D. *J. Am. Chem. Soc.* **1988**, *110*, 5959.
- Xue, C. X.; Cui, S. Y.; Liu, M. C.; Hu, Z. D.; Fan, B. T. *Eur. J. Med. Chem.* **2004**, *39*, 745.
- Niu, Y. Y.; Yang, L. M.; Liu, H. Z.; Cui, Y. Y.; Zhu, L.; Feng, J. M.; Yao, J. H.; Chen, H. Z.; Fan, B. T.; Chen, Z. N.; Lu, Y. *Bioorg. Med. Chem. Lett.* **2005**, *15*, 4814.
- Kulkarni, S. S.; Kopajtic, T. A.; Katz, J. L.; Newman, A. H. *Bioorg. Med. Chem.* **2006**, *11*, 3625.
- Cratteri, P.; Novella Romanelli, M.; Cruciani, G.; Bonaccini, C.; Melani, F. *J. Comput. Aided Mol. Des.* **2004**, *18*, 361.
- Wang, Y. G.; Chackalamannil, S.; Hu, Z. Y.; Clader, J. W.; Greenlee, W.; Billard, W.; Binch, H., III; Crosby, G.; Ruperto, V.; Duffy, R. A.; McQuade, R.; Lachowicz, J. E. *Bioorg. Med. Chem. Lett.* **2000**, *10*, 2247.
- SYBYL 6.9, Tripos Associates, St. Louis, MO, USA, **1999**; <http://www.tripos.com/available> from.
- Billard, W.; Binch, H., III; Bratzler, K.; Chen, L. Y.; Crosby, G., Jr.; Duffy, R. A.; Dugar, S.; Lachowicz, J.; McQuade, R.; Pushpavanam, P.; Ruperto, V. B.; Taylor, L. A.; Clader, J. W. *Bioorg. Med. Chem. Lett.* **2000**, *10*, 2209.
- Kozlowski, J. A.; Lowe, D. B.; Guzik, H. S.; Zhou, G.; Ruperto, V. B.; Duffy, R. A.; McQuade, R.; Crosby, G., Jr.; Taylor, L. A.; Billard, W.; Binch, H., III; Lachowicz, J. E. *Bioorg. Med. Chem. Lett.* **2000**, *10*, 2255.
- Wang, Y. G.; Chackalamannil, S.; Hu, Z. Y.; McKittrick, B. A.; Greenlee, W.; Ruperto, V.; Duffy, R. A.; Lachowicz, J. E. *Bioorg. Med. Chem. Lett.* **2002**, *12*, 1087.
- Wang, Y. G.; Chackalamannil, S.; Chang, W.; Greenlee, W.; Ruperto, V.; Duffy, R. A.; McQuade, R.; Lachowicz, J. E. *Bioorg. Med. Chem. Lett.* **2001**, *11*, 891.
- Tanczos, A. C.; Palmer, R. A.; Potter, B. S.; Saldanha, J. W.; Howlin, B. J. *Comput. Biol. Chem.* **2004**, *28*, 375.
- Johren, K.; Holtje, H. D. *J. Comput. Aided Mol. Des.* **2002**, *16*, 795.
- Selent, J.; Brandt, W.; Pamperin, D.; Göber, B. *Bioorg. Med. Chem.* **2006**, *14*, 1729.
- Han, S. J.; Hamdan, F. F.; Kim, S. K.; Jacobson, K. A.; Bloodworth, L. M.; Li, B.; Wess, J. *J. Biol. Chem.* **2005**, *280*, 34849.
- Hulme, E. C.; Lu, Z. L.; Saldanha, J. W.; Beef, M. S. *Biochem. Soc. Trans.* **2003**, *31*, 29.
- Lu, Z. L.; Saldanha, J.; Hulme, E. C. *J. Biol. Chem.* **2001**, *276*, 34098.